HIGH PRECISION TARGET LOCALIZATION METHOD BASED ON COMPENSATION OF ATTITUDE ANGLE ERRORS

Jialiang Liu[1], Wenrui Ding [1, 2], and Hongguang Li [3]
[1] School of Electronic and Information Engineering, Beijing University of Aeronautics and Astronautics
[2] Collaborative Innovation Center of Geospatial Technology
[3] Research Institute of Unmanned Aerial Vehicle, Beijing University of Aeronautics and Astronautics;
E-Mail: lihongguang@buaa.edu.cn;

Submitted: Nov. 17, 2015 ***Accepted: Jan. 23, 2016*** ***Published: Mar. 1, 2016***

Abstract- The attitude angles of UAV, as the input parameters of the target localization process, influence the accuracy of geo-targeting. In order to improve the accuracy of target localization, this paper compensates the attitude angle errors of the UAV based on learning prediction compensation. Firstly, considering the airborne equipment and the metadata provided by the UAV, we combine rear intersection with GPS/INS to calculate the error of each platform and aircraft attitude angle. Then the error prediction model to compensate each platform and aircraft attitude error is derived by analyzing the error distribution and polynomial regression. Afterwards, because of the limit of the UAV aerial image amount and the similar influence of each attitude angle error on targeting and geometric correction, we use equivalent optical axis angle to represent platform and aircraft attitudes. Furthermore, we also predict and compensate the error of the equivalent angle. In this process, we adopt SVM and regression to classify and obtain error prediction model of equivalent optical axis angle. Finally, the actual data is used to verify the compensation algorithm. The results show that the method can improve the accuracy of target localization efficiently, and has a certain value of engineering guidance and practical application.

Index terms*:* UAV; Geo-targeting technology; Attitude Angles; Rear intersection; Regression; Learning.

I. INTRODUCTION

In recent years, the UAV is widely used in military, agriculture, life and other aspects. UAV geo-targeting technology, one of the important missions of UAV, is the foundation of targeting tracking [1] and surveillance technique, and the positioning accuracy will directly affect the follow-up tasks. However, due to some objective limits, such as installation errors, lower precision of measurement unit, there often exist errors in the sensors of UAV, which deleteriously affects the target positioning accuracy. Therefore, to improve the accuracy of target localization, it is necessary to study how to reduce the attitude angle error of UAV.

In order to improve the accuracy of target localization, domestic and foreign scholars have proposed many improved and innovative models and methods. Expect introducing some other sensors [2], some scholars use multiple images to improve target positioning accuracy. Meir Pachter achieves the purpose by repeatedly targeting the fixed ground object from multiple directions, so as to reduce the random error and systematic error [3]; K. Han and G. N. DeSouza use sift and stereo vision on airborne video sequences to estimate the terrain of target to improve localization accuracy [4]. Using multiple UAVs, J. Tisdale and his group have improved the localization accuracy of a ground target [5]. Some improve the positioning accuracy by eliminating the errors of the aircraft sensors. M. Jensen Austin found and eliminated the inherent errors of the attitude sensors by inverse-orthorectifying images and General Procrustes, thus improving the accuracy of target localization [6]. Myung Hwangbo and Takeo Kanade use a set of line segments in images of urban areas that are either parallel or orthogonal to the gravitational direction to provide visual measurements for the absolute attitude from a calibrated camera [7]. However, because of using multiple images or introducing some extra information and artificial assistance, the methods above do not have good real-time performance.

In addition, some scholars improve the positioning accuracy through compensating the error of interior and exterior orientation parameters [8]. Jun Wu proposes one from coarse to fine calibration method which improves the accuracy of exterior orientation parameters (EoPs) by 5 steps [9]. Najib A. Metni studies the sensor fusion to estimate the orientation accurately [10]. Nevertheless, EoPs are not directly provided by the UAV's metadata. Of course, camera calibration can also be used to raise the accuracy of the sensor, such as the direct linear transformation [11] and two calibration planes [12]. The relative pose and position of the UAV

can also be solved by using artificial icon, such as Amidi et al., with an icon made of 6 rectangles, calculate the relative pose of the UAV by detecting the corner points of all rectangles [13]. However, the sensor error always varies with time, camera calibration too complex to calibrate camera before every flight. What's more, the best way to eliminate the error of aircraft sensor may be use the method of field calibration [14]. Therefore, this paper presents a method to obtain the prediction model of attitude errors with the results of field calibration in advance, which can effectively improve the positioning accuracy but also guarantee the instantaneity.

In view of the above problems, this paper firstly uses the method of field calibration to obtain the error of the platform and aircraft attitude angles. In this process, we combine rear intersection with GPS/INS to calculate the error of each attitude angle directly. Then we analyze the relationship between the error and the attitude angle to acquire the error compensation formula. Finally, by compensating the attitude errors, we can improve the accuracy of target localization in real time.

II. METHODOLOGY

In the process of target localization, which based on the imaging model, the position information and the attitude information of UAV are required as input data. According to the collinear equation, the relation between image pixels coordinates and geographical coordinates are established. Then the position information of the target is obtained according to the proportion of the similar triangles. By analyzing the target localization method based on imaging model, we can see that the accuracy of attitude information of UAV will directly affect the accuracy of target localization. What's more, in the practical application, there is a certain relationship between the accuracy of the target localization and the attitude of the UAV. Assuming that $X_C Y_C Z_C$, $X_P Y_P Z_P$, $X_N Y_N Z_N$ and $X_A Y_A Z_A$ respectively represent Camera platform coordinate, Plane body coordinate, North-East-Up coordinate and space rectangular coordinate. When we define each coordinate system as shown in Figure 1, we can get the relationship between the target localization error and the attitude angle of the UAV shown in Figure 2. Concretely, Figure 2(a) shows the relationship between position error and platform elevation, and Figure 2(b) shows the relationship between position error and platform azimuth. This means the target localization accuracy can be improved by compensating the attitude errors.

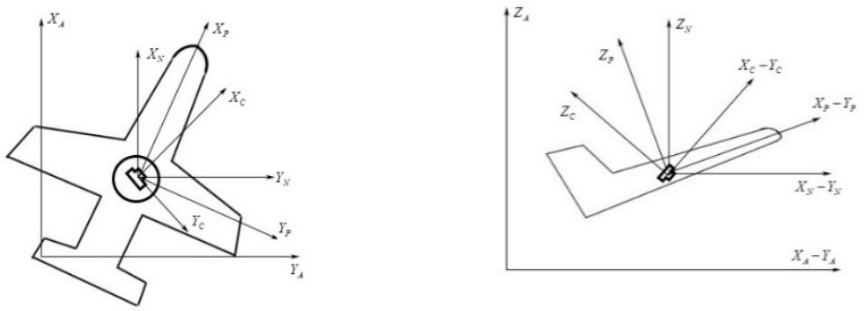

- **Figure 1.** The Schematic Diagram of each Coordinate System

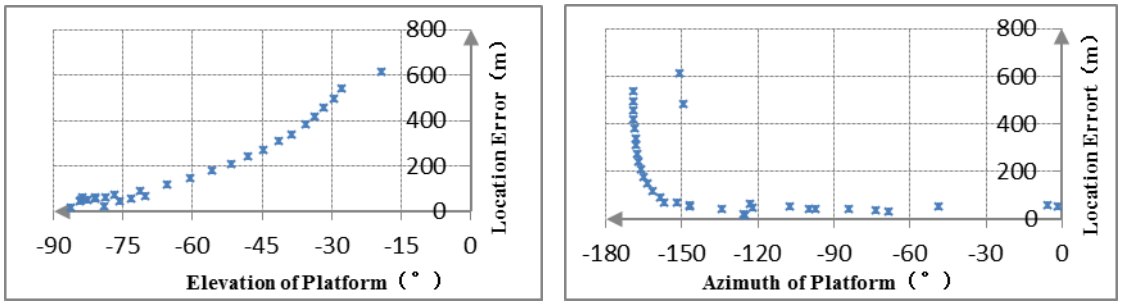

(a) (b)

- **Figure 2.** Relationship between Target Localization Accuracy and the Attitude of UAV

2.1 Compensation Error of Each Attitude Angle

Firstly, we improve the rear intersection to calculate error of each platform attitude angle (platform elevation and platform azimuth) and aircraft attitude angle (aircraft pitch, aircraft roll and aircraft yaw). Then analyze the relationship between the error and the attitude angle to acquire the error compensation formula. Finally carry out target localization with compensated attitude angles to improve the accuracy.

2.1.1 Calculation of Each Attitude Angle Error

On one hand, in order to guarantee the authenticity and availability of the error calculated, we use the field calibration method. On the other hand, in order to use and compensate the metadata provided by UAV directly, we combine rear intersection with GPS/INS. Rear intersection uses the principle of the corresponding relationship between ground control points and image pixel coordinates, linearizes the collinear equation to establish the error equation, and derive the error of each attitude angle value by iteration. First, we use provided telemetry parameters of GPS/INS as the initial values. Then according to the collinearity equation, calculate the camera coordinate

platform corresponding to the ground control points. Afterwards, utilizing the information of multiple control points and repeating the above operations, we can derive error equations and solve them. Finally, by performing several iterations until corrections are less than the tolerance, we can get the value of each attitude angle error.

1) Calculate rotation matrix according to the telemetry parameters

Calculate Rotation matrix with platform parameters (platform azimuth κ_1 and platform elevation ω_1) and aircraft parameters (pitch ϕ_2, roll ω_2 and yaw κ_2). The schematic diagram of each coordinate system is shown in Figure 1.

$$\begin{bmatrix} x_N \\ y_N \\ z_N \end{bmatrix} = R_Z(\kappa_2)R_X(\phi_2)R_Y(\omega_2)R_Z(\kappa_1)R_Y(\omega_1)\begin{bmatrix} x_c \\ y_c \\ -f \end{bmatrix} = R\begin{bmatrix} x_c \\ y_c \\ -f \end{bmatrix} = \begin{bmatrix} a_1 & a_2 & a_3 \\ b_1 & b_2 & b_3 \\ c_1 & c_2 & c_3 \end{bmatrix}\begin{bmatrix} x_P \\ y_P \\ z_P \end{bmatrix} \tag{1}$$

2) According to the collinear equation, calculate the control points' approximate values of the coordinates of the camera platform (x) (y)

Because imaging principle of UAV is the central projection, we can establish the conversion relation from North-East-Up coordinate to space rectangular coordinate system based on collinear equation. Suppose the plane coordinates in space rectangular coordinate system is (X_s, Y_s, Z_s) and Cartesian coordinates of the target point is (X, Y, Z) .The conversion relationship can be expressed as

$$\frac{x_N}{X - X_s} = \frac{y_N}{Y - Y_s} = \frac{z_N}{Z - Z_s} = \frac{1}{\lambda} \tag{2}$$

Instead, we can use the ground control points (GCPs) to obtain coordinates of camera platform according to the collinearity equation of central projection

$$\begin{cases} x_c = -f\dfrac{a_1(X - X_s) + b_1(Y - Y_s) + c_1(Z - Z_s)}{a_3(X - X_s) + b_3(Y - Y_s) + c_3(Z - Z_s)} \\ y_c = -f\dfrac{a_2(X - X_s) + b_2(Y - Y_s) + c_2(Z - Z_s)}{a_3(X - X_s) + b_3(Y - Y_s) + c_3(Z - Z_s)} \end{cases} \tag{3}$$

x_c、 y_c is the approximation of the camera platform coordinates (x) (y) corresponding to the control point.

3) Derive error equation according to the collinear equation

The collinear equation is linearized and takes first small value items

$$\begin{cases} x_c = (x) + \dfrac{\partial x}{\partial X_s} dX_s + \dfrac{\partial x}{\partial Y_s} dY_s + \dfrac{\partial x}{\partial Z_s} dZ_s + \dfrac{\partial x}{\partial \omega_1} d\omega_1 + \dfrac{\partial x}{\partial \kappa_1} d\kappa_1 + \dfrac{\partial x}{\partial \omega_2} d\omega_2 + \dfrac{\partial x}{\partial \phi_2} d\phi_2 + \dfrac{\partial x}{\partial \kappa_2} d\kappa_2 \\ y_c = (y) + \dfrac{\partial y}{\partial X_s} dX_s + \dfrac{\partial y}{\partial Y_s} dY_s + \dfrac{\partial y}{\partial Z_s} dZ_s + \dfrac{\partial y}{\partial \omega_1} d\omega_1 + \dfrac{\partial y}{\partial \kappa_1} d\kappa_1 + \dfrac{\partial y}{\partial \omega_2} d\omega_2 + \dfrac{\partial y}{\partial \phi_2} d\phi_2 + \dfrac{\partial y}{\partial \kappa_2} d\kappa_2 \end{cases} \tag{4}$$

The geodetic coordinates of control points are considered as true value, and the corresponding image point coordinates are considered as observations, in accordance with the principle that observed value +observed value corrections= approximate value + approximate value corrections, so we can derive

$$\begin{cases} x_c + v_x = (x) + dx \\ y_c + v_y = (y) + dy \end{cases} \tag{5}$$

So the error equation for each point can be denoted as

$$\begin{cases} v_x = \dfrac{\partial x}{\partial X_s} dX_s + \dfrac{\partial x}{\partial Y_s} dY_s + \dfrac{\partial x}{\partial Z_s} dZ_s + \dfrac{\partial x}{\partial \omega_1} d\omega_1 + \dfrac{\partial x}{\partial \kappa_1} d\kappa_1 + \dfrac{\partial x}{\partial \omega_2} d\omega_2 + \dfrac{\partial x}{\partial \phi_2} d\phi_2 + \dfrac{\partial x}{\partial \kappa_2} d\kappa_2 + (x) - x_c \\ v_y = \dfrac{\partial y}{\partial X_s} dX_s + \dfrac{\partial y}{\partial Y_s} dY_s + \dfrac{\partial y}{\partial Z_s} dZ_s + \dfrac{\partial y}{\partial \omega_1} d\omega_1 + \dfrac{\partial y}{\partial \kappa_1} d\kappa_1 + \dfrac{\partial y}{\partial \omega_2} d\omega_2 + \dfrac{\partial y}{\partial \phi_2} d\phi_2 + \dfrac{\partial y}{\partial \kappa_2} d\kappa_2 + (y) - y_c \end{cases} \tag{6}$$

If denote the coefficients by $a_{11...}$ a28, the equation above can be written as

$$\begin{cases} v_x = a_{11} dX_s + a_{12} dY_s + a_{13} dZ_s + a_{14} d\omega_1 + a_{15} d\kappa_1 + a_{16} d\omega_2 + a_{17} d\phi_2 + a_{18} d\kappa_2 - l_x \\ v_y = a_{21} dX_s + a_{22} dY_s + a_{23} dZ_s + a_{24} d\omega_1 + a_{25} d\kappa_1 + a_{26} d\omega_2 + a_{27} d\phi_2 + a_{28} d\kappa_2 - l_y \end{cases} \tag{7}$$

where

$$\begin{cases} l_x = x_c - (x) \\ l_y = y_c - (y) \end{cases} \tag{8}$$

And the equation can be written in the form of matrix, which is

$$V = AX - l \tag{9}$$

where

$$\begin{cases} V = \begin{bmatrix} v_x, v_y \end{bmatrix}^{\mathrm{T}} \\ A = \begin{bmatrix} a_{11} & a_{12} & a_{13} & a_{14} & a_{15} & a_{16} & a_{17} & a_{18} \\ a_{21} & a_{22} & a_{23} & a_{24} & a_{25} & a_{26} & a_{27} & a_{28} \end{bmatrix} \\ X = \begin{bmatrix} dX_s & dY_s & dZ_s & d\omega_1 & d\kappa_1 & d\omega_2 & d\phi_2 & d\kappa_2 \end{bmatrix}^{\mathrm{T}} \\ l = \begin{bmatrix} l_x & l_y \end{bmatrix}^{\mathrm{T}} \end{cases} \tag{10}$$

4）Calculate the coefficients of corrections

For simplicity, the numerator and denominator in collinear equation can be denoted by

$$\begin{bmatrix} \overline{X} \\ \overline{Y} \\ \overline{Z} \end{bmatrix} = \begin{bmatrix} a_1 & b_1 & c_1 \\ a_2 & b_2 & c_2 \\ a_3 & b_3 & c_3 \end{bmatrix} \begin{bmatrix} X - X_s \\ Y - Y_s \\ Z - Z_s \end{bmatrix} = R^{\mathrm{T}} \begin{bmatrix} X - X_s \\ Y - Y_s \\ Z - Z_s \end{bmatrix} = R_Y{}^{\mathrm{T}}(\omega_1) R_Z{}^{\mathrm{T}}(\kappa_1) R_Y{}^{\mathrm{T}}(\omega_2) R_X{}^{\mathrm{T}}(\phi_2) R_Z{}^{\mathrm{T}}(\kappa_2) \begin{bmatrix} X - X_s \\ Y - Y_s \\ Z - Z_s \end{bmatrix} \quad (11)$$

Then the coefficients can be calculated as follows

$$\begin{cases} a_{11} = \dfrac{\partial x}{\partial X_s} = \dfrac{1}{\overline{Z}}(a_1 f + a_3 x_c) \\ a_{12} = \dfrac{\partial x}{\partial Y_s} = \dfrac{1}{\overline{Z}}(b_1 f + b_3 x_c) \\ a_{13} = \dfrac{\partial x}{\partial Z_s} = \dfrac{1}{\overline{Z}}(c_1 f + c_3 x_c) \\ a_{14} = \dfrac{\partial x}{\partial \omega_1} = -\dfrac{f}{(\overline{Z})^2}\left(\dfrac{\partial \overline{X}}{\partial \omega_1}\overline{Z} - \dfrac{\partial \overline{Z}}{\partial \omega_1}\overline{X}\right) \\ a_{15} = \dfrac{\partial x}{\partial \kappa_1} = -\dfrac{f}{(\overline{Z})^2}\left(\dfrac{\partial \overline{X}}{\partial \kappa_1}\overline{Z} - \dfrac{\partial \overline{Z}}{\partial \kappa_1}\overline{X}\right) \\ a_{16} = \dfrac{\partial x}{\partial \omega_2} = -\dfrac{f}{(\overline{Z})^2}\left(\dfrac{\partial \overline{X}}{\partial \omega_2}\overline{Z} - \dfrac{\partial \overline{Z}}{\partial \omega_2}\overline{X}\right) \\ a_{17} = \dfrac{\partial x}{\partial \phi_2} = -\dfrac{f}{(\overline{Z})^2}\left(\dfrac{\partial \overline{X}}{\partial \phi_2}\overline{Z} - \dfrac{\partial \overline{Z}}{\partial \phi_2}\overline{X}\right) \\ a_{18} = \dfrac{\partial x}{\partial \kappa_2} = -\dfrac{f}{(\overline{Z})^2}\left(\dfrac{\partial \overline{X}}{\partial \kappa_2}\overline{Z} - \dfrac{\partial \overline{Z}}{\partial \kappa_2}\overline{X}\right) \end{cases} \quad \begin{cases} a_{21} = \dfrac{\partial y}{\partial X_s} = \dfrac{1}{\overline{Z}}(a_2 f + a_3 y_c) \\ a_{22} = \dfrac{\partial y}{\partial Y_s} = \dfrac{1}{\overline{Z}}(b_2 f + b_3 y_c) \\ a_{23} = \dfrac{\partial y}{\partial Z_s} = \dfrac{1}{\overline{Z}}(c_2 f + c_3 y_c) \\ a_{24} = \dfrac{\partial y}{\partial \omega_1} = -\dfrac{f}{(\overline{Z})^2}\left(\dfrac{\partial \overline{Y}}{\partial \omega_1}\overline{Z} - \dfrac{\partial \overline{Z}}{\partial \omega_1}\overline{Y}\right) \\ a_{25} = \dfrac{\partial y}{\partial \kappa_1} = -\dfrac{f}{(\overline{Z})^2}\left(\dfrac{\partial \overline{Y}}{\partial \kappa_1}\overline{Z} - \dfrac{\partial \overline{Z}}{\partial \kappa_1}\overline{Y}\right) \\ a_{26} = \dfrac{\partial y}{\partial \omega_2} = -\dfrac{f}{(\overline{Z})^2}\left(\dfrac{\partial \overline{Y}}{\partial \omega_2}\overline{Z} - \dfrac{\partial \overline{Z}}{\partial \omega_2}\overline{Y}\right) \\ a_{27} = \dfrac{\partial y}{\partial \phi_2} = -\dfrac{f}{(\overline{Z})^2}\left(\dfrac{\partial \overline{Y}}{\partial \phi_2}\overline{Z} - \dfrac{\partial \overline{Z}}{\partial \phi_2}\overline{Y}\right) \\ a_{28} = \dfrac{\partial y}{\partial \kappa_2} = -\dfrac{f}{(\overline{Z})^2}\left(\dfrac{\partial \overline{Y}}{\partial \kappa_2}\overline{Z} - \dfrac{\partial \overline{Z}}{\partial \kappa_2}\overline{Y}\right) \end{cases} \quad (12)$$

Therefore, we have

$$\frac{\partial}{\partial \kappa_2}\begin{bmatrix}\overline{X}\\ \overline{Y}\\ \overline{Z}\end{bmatrix} = R_Y{}^{\mathrm{T}}(\omega_1)R_Z{}^{\mathrm{T}}(\kappa_1)R_Y{}^{\mathrm{T}}(\omega_2)R_X{}^{\mathrm{T}}(\phi_2)\frac{\partial R_Z{}^{\mathrm{T}}(\kappa_2)}{\partial \kappa_2}\begin{bmatrix}X-X_s\\ Y-Y_s\\ Z-Z_s\end{bmatrix}$$

$$\frac{\partial}{\partial \omega_2}\begin{bmatrix}\overline{X}\\ \overline{Y}\\ \overline{Z}\end{bmatrix} = R_Y{}^{\mathrm{T}}(\omega_1)R_Z{}^{\mathrm{T}}(\kappa_1)R_Y{}^{\mathrm{T}}(\omega_2)\frac{\partial R_X{}^{\mathrm{T}}(\phi_2)}{\partial \phi_2}R_Z{}^{\mathrm{T}}(\kappa_2)\begin{bmatrix}X-X_s\\ Y-Y_s\\ Z-Z_s\end{bmatrix}$$

$$\frac{\partial}{\partial \phi_2}\begin{bmatrix}\overline{X}\\ \overline{Y}\\ \overline{Z}\end{bmatrix} = R_Y{}^{\mathrm{T}}(\omega_1)R_Z{}^{\mathrm{T}}(\kappa_1)\frac{\partial R_Y{}^{\mathrm{T}}(\omega_2)}{\partial \omega_2}R_X{}^{\mathrm{T}}(\phi_2)R_Z{}^{\mathrm{T}}(\kappa_2)\begin{bmatrix}X-X_s\\ Y-Y_s\\ Z-Z_s\end{bmatrix}$$

$$\frac{\partial}{\partial \kappa_1}\begin{bmatrix}\overline{X}\\ \overline{Y}\\ \overline{Z}\end{bmatrix} = R_Y{}^{\mathrm{T}}(\omega_1)\frac{\partial R_Z{}^{\mathrm{T}}(\kappa_1)}{\partial \kappa_1}R_Y{}^{\mathrm{T}}(\omega_2)R_X{}^{\mathrm{T}}(\phi_2)R_Z{}^{\mathrm{T}}(\kappa_2)\begin{bmatrix}X-X_s\\ Y-Y_s\\ Z-Z_s\end{bmatrix}$$

$$\frac{\partial}{\partial \omega_1}\begin{bmatrix}\overline{X}\\ \overline{Y}\\ \overline{Z}\end{bmatrix} = \frac{\partial R_Y{}^{\mathrm{T}}(\omega_1)}{\partial \omega_1}R_Z{}^{\mathrm{T}}(\kappa_1)R_Y{}^{\mathrm{T}}(\omega_2)R_X{}^{\mathrm{T}}(\phi_2)R_Z{}^{\mathrm{T}}(\kappa_2)\begin{bmatrix}X-X_s\\ Y-Y_s\\ Z-Z_s\end{bmatrix} \tag{13}$$

5）Obtain normal equations by calculating for each control point

If the number of control points is n, we can list n groups of error equations $\begin{bmatrix}V_1 & V_2 & \cdots & V_n\end{bmatrix}^{\mathrm{T}}$, and form the total error equation as

$$V = AX - L \tag{14}$$

where

$$\begin{cases} V = \begin{bmatrix}V_1 & V_2 & \cdots & V_n\end{bmatrix}^{\mathrm{T}} \\ A = \begin{bmatrix}A_1 & A_2 & \cdots & A_n\end{bmatrix}^{\mathrm{T}} \\ L = \begin{bmatrix}l_1 & l_2 & \cdots & l_n\end{bmatrix}^{\mathrm{T}} \end{cases} \tag{15}$$

In the light of the least squares principle of indirect adjustment, we can derive the normal equation as

$$A^{\mathrm{T}}AX = A^{\mathrm{T}}L \tag{16}$$

Then the vector solution can be obtained

$$X = (A^{\mathrm{T}}A)^{-1}A^{\mathrm{T}}L \tag{17}$$

That is to say, we can gain the corrections $dX_s, dY_s, dZ_s, d\omega_1, d\kappa_1, d\omega_2, d\phi_2, d\kappa_2$。

6）Obtain the final error by iterating until corrections is less than the tolerance

Compare the correction obtained each time with the tolerance. If the requirement is not met, perform the iteration until the correction is less than the tolerance. Finally, we obtain the total error of each attitude angle.

2.1.2 Compensation of Each Attitude Angle Error

According to rear intersection, the error distribution of each attitude angle can be calculated. Through the analysis of the experimental data, the error of the attitude angle is distributed according to a certain trend. Therefore, the error prediction model can be established through the study of attitude angle error. After the wrong data are removed, we can use the least square method to carry out regression study, and then get the prediction model of each attitude angle error.

In order to improve the real-time performance and reduce the amount of data required in flight, the basic form of error prediction model is obtained by analyzing the error distribution of previous flight test data. Then modify the parameters using a small amount of the flight data, so as to make use of the prediction model to forecast and compensate the error of each attitude angle. At last, the target position is calculated after the compensation of the attitude angle. Figure 3 shows the flow chart of platform and aircraft attitude angle error compensation.

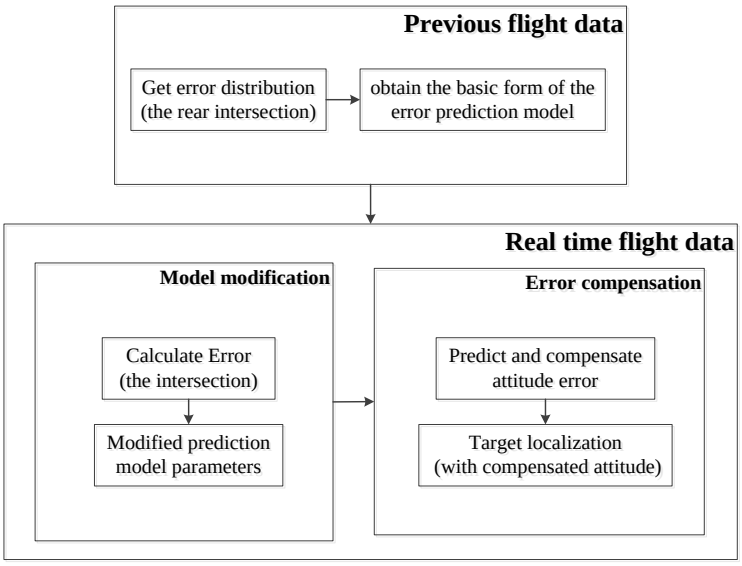

- **Figure 3.** Flow Chart of Platform and Aircraft Attitude Angle Error Compensation

2.2 Compensation Errors of Equivalent Angle

However, because of the limit of the UAV aerial image amount, previous flight data is difficult to cover every range of platform and aircraft attitude angle. In order to improve the localization accuracy efficiently with limited training set, it is necessary decrease the number of attitude angles to be compensated. Therefore, using the method of combining theoretical analysis and experimental data, we equal the platform and aircraft attitudes to equivalent optical axis angle. Then calculate and compensate the error of equivalent optical axis angle to improve targeting accuracy.

2.2.1 Angle Equivalence and Calculation of Equivalent Angle Error

By analyzing the target localization method based on the imaging model and experimental data, we can draw some conclusions about the influence of each platform and aircraft attitude angle error.

On one hand, the influence of the platform elevation error and the aircraft pitch error on the displacement of the final target is similar, and the direction of the displacement is the optical axis direction. The influence of the platform azimuth error the platform yaw error on the displacement of the final target is similar, and the displacement direction is perpendicular to the direction of the optical axis.

On the other hand, the error of platform elevation and the error of aircraft pitch have approximately effect on the final geometric correction; they both will produce a scaling transformation for the final corrected image. The error of platform azimuth and the error of aircraft yaw have approximately similar effect on the final geometric correction; they both will produce a rotation transformation for the final corrected image. Although the roll error will produce a cut transformation on the final geometric correction, the roll angle of UAV is usually small, and it has little influence on the optical axis.

Therefore, the platform elevation and the aircraft pitch can be equivalent to the optical axis lip angle, and the platform azimuth and the aircraft yaw can be equivalent to the optical axis direction angle. Figure 4 shows the schematic diagram of the optical axis angle. The optical axis lip angle is represented by $d\rho$, and the optical axis direction angle is represented by $d\theta$.

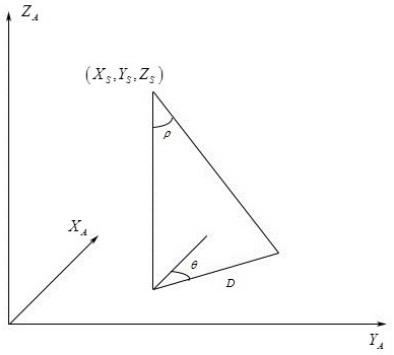

- **Figure 4.** Schematic Diagram of the Angle Error and the Optical Axis Angle

So the equivalent angle error can be calculated as

$$\begin{cases} d\theta = d\kappa_1 + d\kappa_2 \\ d\rho = d\omega_1 - d\omega_2 \\ d\phi_2 = d\phi_2 \end{cases} \tag{18}$$

2.2.2 Compensation of Equivalent Angle Error

However, the experimental results show that we cannot simply use an error prediction formula to represent the error distribution. As is shown in Figure 5, when the optical axis lip/direction angle is same, the corresponding errors may appear two different trends. In the process of calculating the equivalent optical axis angular error, since the platform error is superimposed with the aircraft error, the equivalent optical axis may have a variety of possible errors at the same angle.

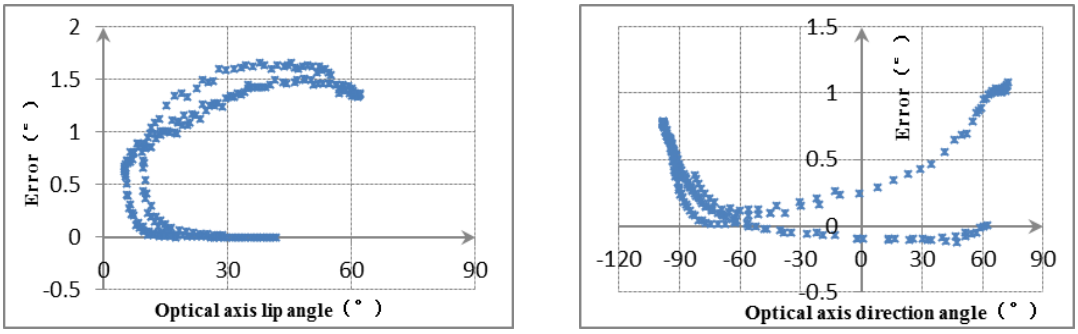

(a) (b)

- **Figure 5.** The Relationship between the Angle Error and the Optical Axis Angle

Figure 5 (a) shows the corresponding relationship between the angle error and the optical axis lip angle. In 0°~40°that two different error trends appear at the same angle. Figure 5(b) shows the error distribution of the equivalent optical axis direction angle. Also in a certain range,

the same optical axis direction angle will correspond to a number of errors. However, different from the lip angle error showing two distinct trends in the opposite direction, the optical axis direction angle error increases with the angle increasing. Thus, it is of great importance to solve the trend classification of lip angle error.

Since the error may be related to multiple attitude angles, and the two kinds of trends are explicit, the error trend can be classified by support vector machines (SVM). First, divide the error of lip, which has two values into two categories. Classification results is marked as 1when the error which is greater than 0.5°increases with the lip increasing, and classification results is marked as 0 when the error which is less than 0.5°decreases with the increase of the lip. Treat aircraft and platform attitudes as input data, 1/0 as the classification results, and adopt SVM training and obtain the required two types of classifiers. Finally, combining with the experimental data, the error prediction model based on actual attitude information is obtained. Figure 6 shows the flow char of error compensation of equivalent optical axis angle based on SVM.

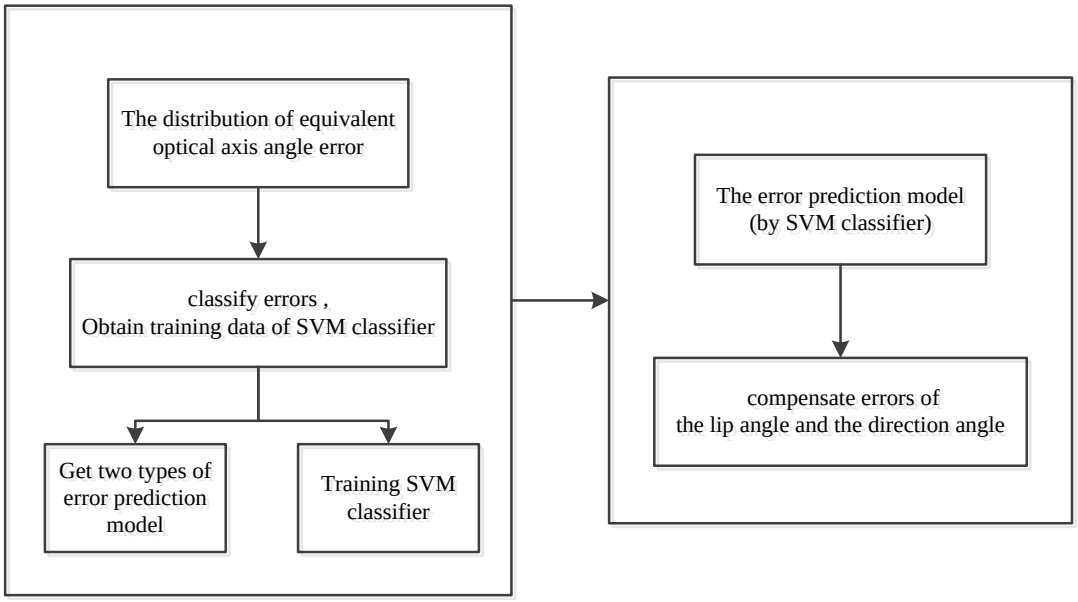

- **Figure 6.** Error Compensation of Equivalent Optical Axis Angle Based on SVM

Then using the error prediction model got from the SVM based on platform and aircraft attitudes, we can compensate the equivalent optical axis angle errors, in order to improve the targeting accuracy.

As can be seen from the above analysis, the impact of aircraft roll error on targeting is different from other attitudes, and the aircraft roll angle is generally floating in the smaller range of. So firstly, compensate the roll error alone, and use the basic objectives positioning theory to

calculate the corrected image. Secondly, compensate the optical axis lip angle and the optical axis direction angle, and use the air triangle and UAV's GPS to get latitude and longitude of the image center point. Finally, the latitude and longitude of the whole image are compensated by the idea of differential. The flow chart is shown in Figure 7.

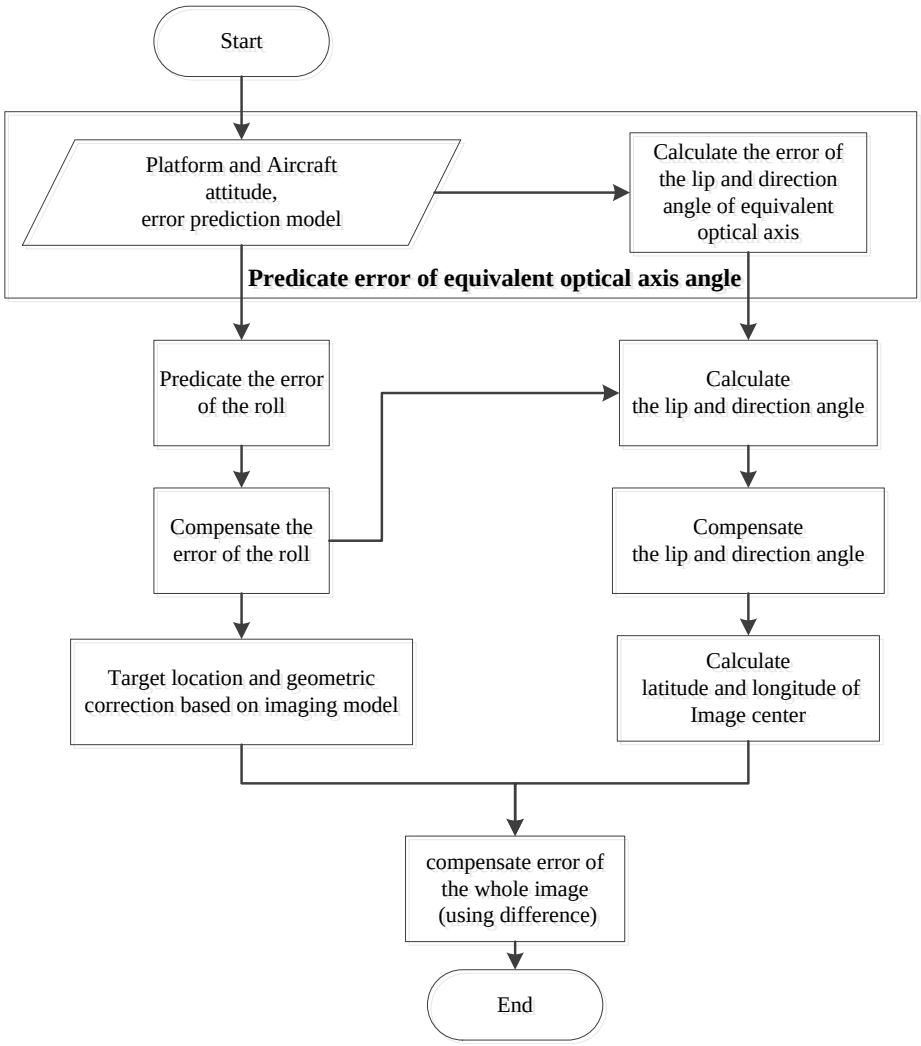

- **Figure 7.** Flow Chart of Equivalent Optical Axis Error Compensation

1) Compensate the roll angle error of UAV, and carry out geometric correction and targeting based on imaging model.

According to the experimental statistics, the mean value of the roll angle error is obtained as the compensation value. Compensate the roll angle of the UAV, and get the rotation matrix R with the original telemetry parameters. Then according to the collinear equation, calculate the geographic coordinates of the center of the image (X, Y).

2) Calculate the optical axis lip angle and the optical axis direction angle, and predict and compensate the error.

According to the relationship between the image and other coordinate systems when the platform and the UAV are in the starting position, it can be assumed that the optical axis of the camera platform coordinates is $(0,0,-f)^{\mathrm{T}}$. So the coordinates of the optical axis in the North-east-Up coordinate system is

$$\begin{bmatrix} x_{Ng} \\ y_{Ng} \\ z_{Ng} \end{bmatrix} = R \begin{bmatrix} 0 \\ 0 \\ -f \end{bmatrix} \tag{19}$$

According to the physical meaning of the optical axis, the optical axis lip angle ρ and the optical axis direction angle θ can be obtained

$$\rho = \mathrm{atan}\left(\frac{\sqrt{x_{Ng}{}^2 + y_{Ng}{}^2}}{|z_{Ng}|}\right) \tag{20}$$

$$\theta = \begin{cases} 90^\circ - \mathrm{atan}\left(\dfrac{x_{Ng}}{y_{Ng}}\right) & x_{Ng} > 0, y_{Ng} > 0 \\ 90^\circ + \mathrm{atan}\left(\dfrac{x_{Ng}}{y_{Ng}}\right) & x_{Ng} < 0, y_{Ng} > 0 \\ -90^\circ - \mathrm{atan}\left(\dfrac{x_{Ng}}{y_{Ng}}\right) & x_{Ng} < 0, y_{Ng} < 0 \\ -90^\circ + \mathrm{atan}\left(\dfrac{x_{Ng}}{y_{Ng}}\right) & x_{Ng} > 0, y_{Ng} < 0 \end{cases} \tag{21}$$

Then according to the experimental statistics and the forecast model obtained by regression learning, we can compensate ρ and θ.

3) Target localization based on aerial triangle with the optical axis lip and the optical axis direction after compensation.

Figure 4 gives a schematic diagram of the basic principle of the air triangle. Set the aircraft position coordinate as (X_s, Y_s, Z_s), the distance projected on the ground between the plane and the target point can be obtained by using the optical axis lip angle $D = Z_S * \tan(\rho)$. Then we can get the coordinates of the center point of the image

$$\begin{cases} X' = X_S + D * \cos(\theta) \\ Y' = Y_S + D * \sin(\theta) \end{cases} \tag{22}$$

4) Differential compensation for the whole image

The difference between geographical coordinates of image center points, which are respectively calculated with the telemetry parameters before and after compensation, can reflect the positioning error of the whole image in a certain extent. Therefore, use difference principle to compensate the rest of the geographic coordinates of the image.

$$\begin{cases} \Delta X = X' - X \\ \Delta Y = Y' - Y \end{cases} \tag{23}$$

III. RESULT AND DISCUSSION

3.1 Analysis of Each Attitude Angle Error

Through the rear intersection, the error information of each attitude angle can be obtained by using the attitude information of UAV as the initial value. A sequence of images is carried out to obtain the error distribution. The error prediction expressions are obtained by polynomial regression, and the errors of the attitude angles are analyzed.

Figure 8 shows the distribution of the platform elevation error, and the change range of the platform elevation is $[-90^\circ, 0^\circ]$. It is obvious that the relationship of elevation and the error of the elevation are nonlinear. The result of quadric polynomial fitting is given. It can be seen that the error is rapidly changing when the platform angle is close to -90° and 0°, and the error in the range of $[-70^\circ, -20^\circ]$ is maintained at about 0.6°. Thus, the error of platform elevation can also be represented with piecewise function.

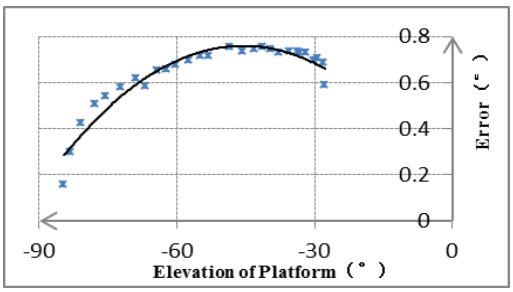

- **Figure 8.** Platform Elevation Error Distribution

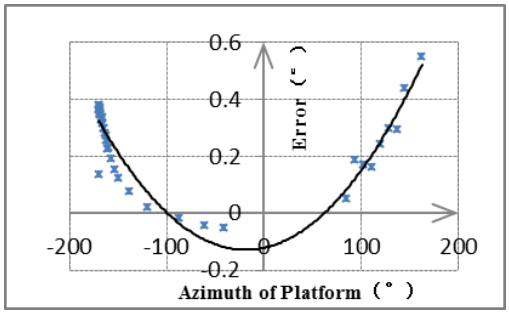

- **Figure 9.** Platform Azimuth Error Distribution

Figure 9 shows the distribution of the platform azimuth error, and the change range of the platform azimuth is $[-180^{\circ},180^{\circ}]$. It can be seen that the relationship between the error of the azimuth angle and the azimuth angle of the platform can be fitted with the quadric polynomial fitting. The quadric polynomial fitting is given, which has a large correlation coefficient. The general trend is that the error is smaller in the vicinity of the 0°, and larger in the vicinity of the $\pm 180^{\circ}$.

Figure 10 shows the relationship between the error of the pitch angle and the pitch angle of the aircraft. Although the actual range of the aircraft pitch angle is $[0^{\circ},90^{\circ}]$, but in the process of the plane stationary flight, the pitch angle is generally active in a smaller range, so here only the error of the pitch in $[0.5^{\circ},2^{\circ}]$ is analyzed. From the graph, we can see that a linear expression can fit the relationship between the pitch angle error and the pitch angle.

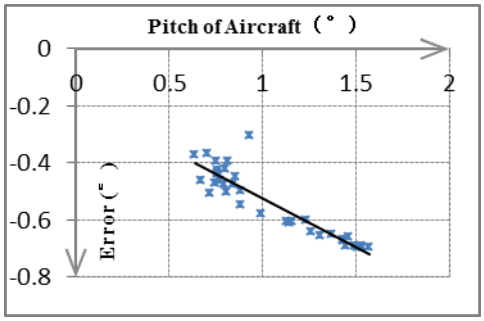

- **Figure 10.** Aircraft Pitch Angle Error Distribution

The relationship between the roll angle error of the plane and the roll angle is shown in Figure 11. Similar to the plane pitch angle, the plane roll angle only varies in a small range in the process of plane stationary flight. Here we only study the distribution of the roll error when roll varies in $[-0.6^{\circ},0.4^{\circ}]$. In the graph, the linear regression and the quadric polynomial regression

are tried, but the correlation coefficient of the regression is not high. This is due to the influence of external factors, such as the horizontal wind. However, the error of the roll angle of the plane is mainly in the range of $\left[0.2^{\circ}, 0.45^{\circ}\right]$. Therefore, the average error data can be used to compensate the roll angle.

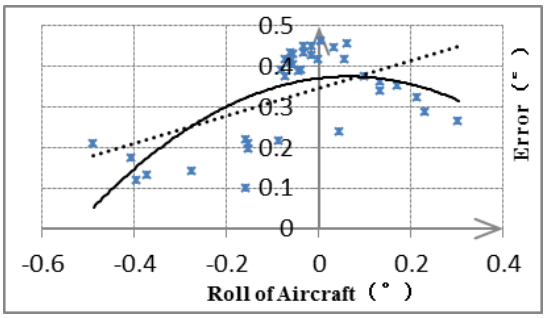

- **Figure 11.** Aircraft Roll Error Distribution

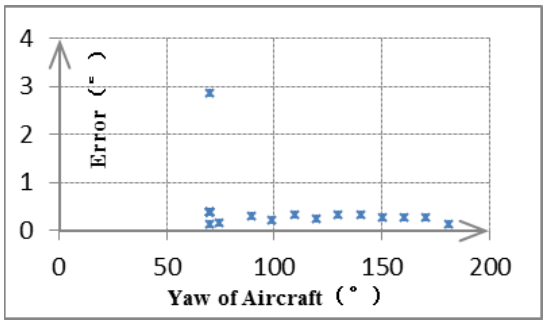

- **Figure 12.** Aircraft Yaw Error Distribution

The range of the yaw angle of the plane should be $\left[0^{\circ}, 360^{\circ}\right]$, but due to the limited data, only the error distribution within $\left[70^{\circ}, 180^{\circ}\right]$ is given in the Figure 12. Nonetheless, it can be seen from the data that the error of the yaw angle of the aircraft is about 0.3°. Therefore, the yaw error can be treated as a constant.

3.2 Analysis of Equivalent Angle Error

The elevation angle error of the platform and the pitch angle error of the aircraft are approximately equivalent to the lip angle error of the optical axis, and the azimuth angle error of the platform and the yaw angle error of the aircraft are approximately equivalent to the direction angle error of the optical axis. By polynomial regression, the approximate error expressions are obtained.

With the increase of the actual situation of the UAV, the error of the equivalent optical axis angle may have two trends. In this case, we cannot obtain a satisfying result using a single error prediction function. So with the introduction of the trained SVM classifier, a suitable error prediction model can be selected based on the attitude of the UAV, so as to further improve the positioning accuracy. Figure 13 shows the classification results of the two trends of equivalent optical axis lip angle error and their predictive models obtained by regression.

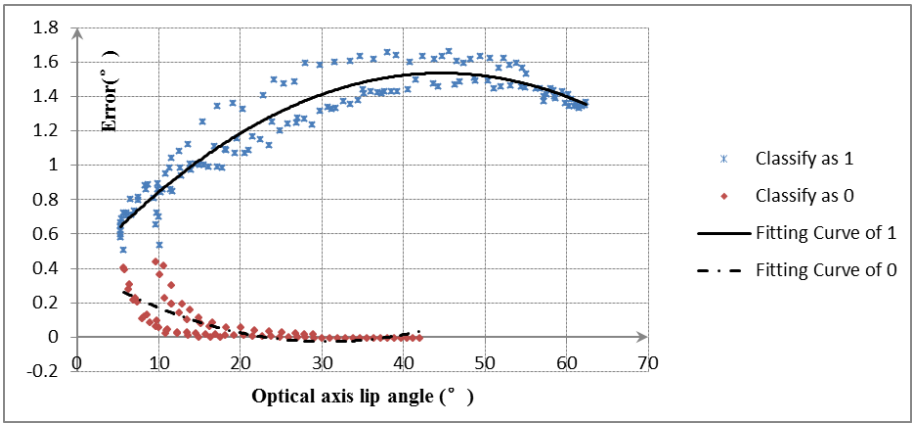

- **Figure 13.** Error Distribution of Optical Axis Angle

3.3 Analysis of Experimental Results

In this experiment, the accuracy of the three methods is compared, i.e. geo-targeting based on imaging model, compensation error of each attitude angle and compensation errors of equivalent angle. According to the above method, we can get the compensation formula of aircraft and platform attitude angle error and equivalent optical axis angle.

In experiment 1, we compensate the remote sensing data when the training set is large enough to cover the change range of each attitude angle. Figure 14 gives a comparison of the results of the experiments. It can be seen that both two kinds of compensation methods have a great improvement in the accuracy of the positioning method, and the positioning accuracy of the two methods is similar. The method of compensating each attitude angle error is a litter better.

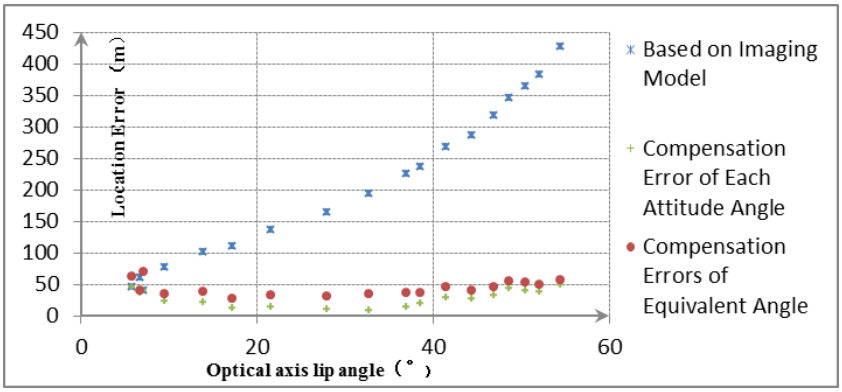

- **Figure 14.** Target Localization Accuracy of Experiment 1

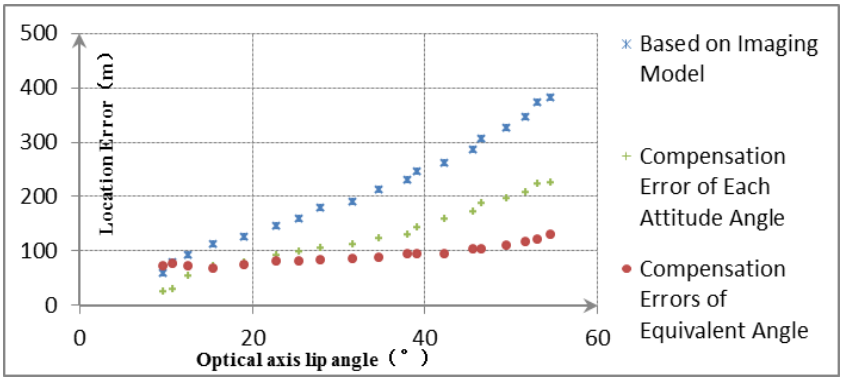

- **Figure 15**. Target Localization Accuracy of Experiment 2

In experiment 2, we use another test set whose attitude angles not all change in the range of the training set. Then we compensate attitude angles with the same error prediction formula with experiment 1.Figure 15 shows the results of the target localization accuracy. In this case, the method of compensating equivalent optical axis angle errors works better.

Table 1 gives the training range and the corresponding angle range of two experiments. From the table, we can see that the two methods are similar in the compensation effect when the test set is concentrated in the training set, and the results of the error compensation of the optical axis are better when the test set is out of the range of the training set.

- **Table 1.** Attitude Angle Range of Experiments

	Elevation of platform	Azimuth of platform	Roll of aircraft	Pitch of aircraft	Yaw of aircraft
Training Set	(-84,-27)	(-170,-20)	(0.6,1.7)	(5,62)	(-98,52)
Experiment 1	(-84,-27)	(-170,-41)	(0.6,1.7)	(5,62)	(-97,32)
Experiment 2	(-80,-35)	(-22,157)	(0.7,2.3)	(9,55)	(-61,72)

In summary, compensation of platform and plane attitude error and compensation of equivalent optical axis error can both improve the accuracy of target localization greatly. Nevertheless, the latter has better generalization ability, and has better robustness to the change of attitude angle.

IV. CONCLUSIONS

By analyzing the target localization method based on imaging model, we can see that the attitude angle error will directly affect the accuracy of the target localization. By combining rear intersection with GPS/INS, we can calculate the angle error of platform and aircraft attitudes. In addition, by analyzing the error distribution and polynomial regression, we can establish the error prediction model of each platform and aircraft attitude. Then we can improve the accuracy of the target localization with compensated platform and aircraft attitudes.

Moreover, based on the influence of every attitude angle error on the final position and correction, the attitude angles of platform and aircraft are equivalent to the lip angle of the optical axis and the direction angle of the optical axis. This is an effectual method when the UAV aerial image amount is limited. In this process, the error prediction models of equivalent optical axis angles are obtained by using SVM and regression.

From the experiments at the end of this paper, we can conclude that the error compensation method of each attitude angle and that of the equivalent effective optical axis angle can both improve the accuracy of target localization largely. When the training set is abundant enough to cover the range of the platform and aircraft attitude angle, both of the two compensation methods can gain good results. While the equivalent optical axis angle method has better adaptive ability and better robustness in the case of small training sets.

AKNOWLEDGEMENT

This work has been supported by the National Natural Science Foundation of China (NO. 61450008).

REFERENCES

[1]HD Yang and Wei Li, “Performance measurement of photoelectric detection and target tracking algorithm [J],” International Journal on Smart Sensing and Intelligent systems VOL. 8, NO. 3, September 2015, pp.1554-1575

[2]BH Shen and GL Wang, “Distributed target localization and tracking with wireless pyroelectric sensor networks [J],” International Journal on Smart Sensing and Intelligent systems VOL. 6, NO. 4, September 2013, pp. 1400 – 1418

[3]M. Pachter, N. Ceccarelli and P. R. Chandler, “Vision-based target geo-location using camera equipped MAVs [J],” in Proc. 46th IEEE Conference on Decision and Control, 2007, pp.2333-2338

[4]K. Han and G. N. DeSouza, “Multiple targets geolocation using sift and stereo vision on airborne video sequences [J],” in 2009 IEEE/RSJ International Conference on Intelligent Robots and Systems, St. Louis, MO, USA, October 2009, pp. 5327-5332.

[5] J. Tisdale, A. Ryan, Z. Kim, D. Tornqvist, and J. K. Hedrick, “A multiple UAV system for vision-based search and localization[C],” in Proc. Amer. Control Conf., Jun. 11–13, 2008, pp. 1985–1990.

[6] A. M. Jensen, N. Wildmann, YQ Chen, and H. Voos, “In-situ unmanned aerial vehicle (UAV) sensor calibration to improve automatic image orthorectification[J],” in Proc. IEEE Int. Geoscience and Remote Sensing Symp. (IGARSS), 2010, pp. 596–599

[7]M. Hwangbo and T. Kanade, “Visual-inertial UAV attitude estimation using urban scene regularities [J],” in: Proceedings of IEEE international conference on robotics and automation. Shanghai, China: IEEE; May.9–13, 2011. pp. 2451–2458.

[8] CF Chen, LY Chang and SR Yang, “Method of calibrating interior and exterior orientation parameters[P].” 2012

[9]W. Jun and G. Zhou. “Calibration of small and low-cost UAV video system for real-time planimetric mapping [C],” IGARSS’06, Denver, Colorado, 2006.

[10]NA. Metni and Z. Mosbeh Lebanon, “Sensor fusion for attitude and bias estimation for a VTOL UAV [C],” proceedings of the ASME 2010 10th Biennial Conference on Engineering Systems Design and Analysis，ESDA2010，July. 12-14, 2010. pp. 363-368

[11]YI Abdel-Aziz and HM Karara. “Direct linear transformation into object space coordinates in close-range photogram-me try [P].” in: Proc. Symp. Close-Range Photogrammetry. 1971. pp. 1-18

[12]HA Martins, JR Birk and RB Kelley, “Camera models based on data from two calibration planes [P].” Computer Graphics and Imaging Processing.1981. pp. 173-180

[13]O. Amidi, T. Kanade R. Miller, “Vision-based autonomous helicopter research at Carnegie Mellon Robotics Institute 1991-1997 [C],” in International Conference on American Helicopter Society, Washington DC, AHS, 1998. pp. 375-386.

[14]AM Jensen, Y Han and YQ Chen, “Using aerial images to calibrate the inertial sensors of a low-cost multispectral autonomous remote sensing platform(AggieAir)[J],” in Proc.IEEE International Conference on Geoscience and Remote Sensing Symposium IGARSS 2009, July. 12-17, 2009. pp. 555 -558